


# Modeling the performance of perovskite solar cells with inserting porous insulating alumina nanoplates

Zhaoyao Pan(潘赵耀), Jinpeng Yang(杨金彭), and Xiaoshuang Shen(沈小双)
**Citation:**Chin. Phys. B, 2024, 33 (**3**): 038501. DOI: 10.1088/1674-1056/ad1480
Journal homepage: http://cpb.iphy.ac.cn; http://iopscience.iop.org/cpb

**What follows is a list of articles you may be interested in**

---

## Large-area fabrication: The next target of perovskite light-emitting diodes

Hang Su(苏杭), Kun Zhu(朱坤), Jing Qin(钦敬), Mengyao Li(李梦瑶), Yulin Zuo(左郁琳), Yunzheng Wang(王允正), Yinggang Wu(吴迎港), Jiawei Cao(曹佳维), and Guolong Li(李国龙)
Chin. Phys. B, 2021, 30 (**8**): 088502. DOI: 10.1088/1674-1056/ac05a4

## Metal halide perovskite photodetectors: Material featuresand device engineering

Ye Wang(王烨), Meng-Lei Gao(高孟磊), Jin-Liang Wu(吴金良), Xing-Wang Zhang(张兴旺)
Chin. Phys. B, 2019, 28 (**1**): 018502. DOI: 10.1088/1674-1056/28/1/018502

## Real-space observation of individual skyrmions in helimagnetic nanostripes

Jin Chi-Ming (金驰名), Du Hai-Feng (杜海峰)
Chin. Phys. B, 2015, 24 (**12**): 128501. DOI: 10.1088/1674-1056/24/12/128501

## Progress and prospects of GaN-based LEDs using nanostructures

Zhao Li-Xia (赵丽霞), Yu Zhi-Guo (于治国), Sun Bo (孙波), Zhu Shi-Chao (朱石超), An Ping-Bo (安平博), Yang Chao (杨超), Liu Lei (刘磊), Wang Jun-Xi (王军喜), Li Jin-Min (李晋闽)
Chin. Phys. B, 2015, 24 (**6**): 068506. DOI: 10.1088/1674-1056/24/6/068506

## Enhanced light emission from InGaN/GaN quantum wells by using surface plasmonic resonances of silver nanoparticle array

Chen Zhan-Xu (陈湛旭), Wan Wei (万巍), Zhang Bai-Jun (张佰君), He Ying-Ji (何影记), Jin Chong-Jun (金崇君)
Chin. Phys. B, 2014, 23 (**12**): 128504. DOI: 10.1088/1674-1056/23/12/128504

---

# Modeling the performance of perovskite solar cells with inserting porous insulating alumina nanoplates

Zhaoyao Pan(潘赵耀), Jinpeng Yang(杨金彭), and Xiaoshuang Shen(沈小双)[†]

*College of Physical Science and Technology, Yangzhou University, Yangzhou* 225009, *China*

(Received 15 September 2023; revised manuscript received 17 November 2023; accepted manuscript online 12 December 2023)

Peng *et al.* [*Science* **379** 683 (2023)] reported an effective method to improve the performance of perovskite solar cells by using thicker porous insulator contact (PIC)-alumina nanoplates. This method overcomes the trade-off between the open-circuit voltage and the fill factor through two mechanisms: reduced surface recombination velocity and increased bulk recombination lifetime due to better perovskite crystallinity. From arguments of drift-diffusion simulations, we find that an increase in mobility and carrier recombination lifetime in bulk are the key factors for minimizing the resistance-effect from thicker PICs and achieving a maximum power conversion efficiency (PCE) at approximately 25% reduced contact area. Furthermore, the partially replacement of perovskite films with thicker PICs would result in a reduction in short-current density, but the relative low refractive index of the PICs imbedded into the high refractive index perovskite creates light trapping structures that compensate for this loss.

**Keywords:** perovskite solar cells, nanostructure, crystalline, mobility

**PACS:** 85.30.De, 73.50.Pz, 78.20.Bh **DOI:** 10.1088/1674-1056/ad1480

## 1. Introduction

Perovskite solar cells exhibit excellent optoelectronic properties. Still, understanding the remaining losses caused by defects is crucial for enhancing device performance. To address this issue, one common approach is to employ various materials to form ultrathin layers (with a thickness of several nanometers) that can passivate the perovskite interfaces, thus resolving the trade-off between open-circuit voltage ($V_{oc}$) and fill factor (FF). Peng *et al.* achieved an $\sim 11\%$ improvement in power efficiency conversion (PEC) for perovskite solar cells by employing a thicker passivating layer of $\sim 100$ nanometer porous insulator contact (PIC) with alumina nanoplates ($Al_2O_3$).[1] They also used drift-diffusion simulations to support their claim that increased coverage leads to greater improvements in device performance (refer to Figs. 1 and S3 in Ref. [1]). In particular, it is noteworthy that only the short-current density ($J_{sc}$) remains almost unchanged as the coverage increases. This raises a natural question: Could increasing the coverage of PIC lead to better PEC in perovskite solar cells? In general, higher coverage of $Al_2O_3$-based PICs can influence the performance of the device in three major ways. Firstly, thick $Al_2O_3$ structures have low conductivities, and their inclusion in perovskite films can reduce the surface area available for carrier transport channels leading to a reduction in $J_{sc}$ and FF (if the mobility of perovskite films remains unchanged). Secondly, partially replacing light-absorbing perovskite films with non-absorbing PICs may result in reduced $J_{sc}$ due to a decrease in the total volume of perovskite films. Lastly, surface defects at the perovskite/hole transporting layers may be diminished by defects passivation since the contact areas after inserting insulating PICs are reduced, which would result in increased $V_{oc}$. After considering all these points of view, it is expected that a proposed maximum PEC will be found at a certain surface coverage fraction. Our numerical simulations have demonstrated that perovskite solar cells cannot be continuously improved by increasing the surface coverage fraction using PIC (as was shown in Ref. [1]). The increase in PEC of perovskite solar cells is primarily a result of improved perovskite crystallinity, which leads to higher bulk mobility and carrier recombination lifetime. Additionally, the low refractive index grid in nanostructured PICs with $Al_2O_3$ promotes photon recycling effects, thereby enhances the perovskite film absorption and resulting in nearly unchanged $J_{sc}$.

## 2. Calculation methods

Figure 1 depicts the establishment of a 3D PIC model in COMSOL Multiphysics, which was simulated by solving the conventional drift-diffusion equations as described in the previous studies.[1–3] To prevent tunneling or electrical injection through the dielectric layer, an insulating boundary condition was set for the PIC structure, and ohmic contacts were assumed at the metal–semiconductor interfaces throughout the calculation process. Aside from the common parameters listed by Peng *et al.* (also see Table S1 in the supplementary materials of the article), we also take into account other factors to ensure that our calculations closely match real-experimental conditions. These considerations include: (i) factoring in the transmission of ITO into our calculations [see Fig. S1(a)]; (ii) defining the absorption coefficients of $FA_{0.95}MA_{0.05}Pb(I_{0.98}Br_{0.02})_3$ using $\alpha(\lambda) = 4\pi\kappa(\lambda)/\lambda$,

[†]Corresponding author. E-mail: xsshen@yzu.edu.cn

© 2024 Chinese Physical Society and IOP Publishing Ltd 

where $\kappa(\lambda)$ is obtained from Ref. [4] and is the imaginary part of the refractive index [see Fig. S1(b)]; and (iii) defining photon generation rate as $\varphi(\lambda) = \lambda/hc \times \mathrm{F}(\lambda)$, with $F(\lambda)$ representing the intensity of AM 1.5 G spectrum [see Fig. S1(c)]. Thus, the integral expression for photo-generation rate under illuminated light can be given as follows:

$$\mathrm{G}(z) = \int_0^\infty \alpha(\lambda)\varphi(\lambda)\exp(-\alpha(\lambda)z)\mathrm{d}\lambda; \qquad (1)$$

(iv) the n-type perovskite films ($N_d = 1 \times 10^{16}$ cm$^{-3}$) are considered instead of author's given parameters (dopant defect concentration with p-type, $N_a = 1 \times 10^{16}$ cm$^{-3}$) in their Table S3 due to published results from photoemission spectroscopy giving a common understanding of n-type behavior;[5–7] and (v) the nano-structured PICs with low refractive index (real part) that induce light trapping and enhance light absorption in perovskite films are also considered (see Fig. S2). In addition, the enhanced crystallinity of perovskite films upon PICs insertion would not only address the defects present at perovskite/hole transporting layer interfaces but also improve carrier lifetime and mobility. We assume a simple linear relationship between mobility ($\mu$) and carrier recombination lifetime ($\tau_b$), as both are influenced by bulk defects ($\mu \propto 1/N_t$ and $\tau_b \propto 1/N_t$).[8–10] For simplicity, perovskite solar cells with non-PICs, we set $\mu = 0.1$ cm$^2$/V·s and $\tau_b = 1$ μs, while for those with PICs, we use $\mu = 0.5$ cm$^2$/V·s and $\tau_b = 5$ μs both for electrons and holes.

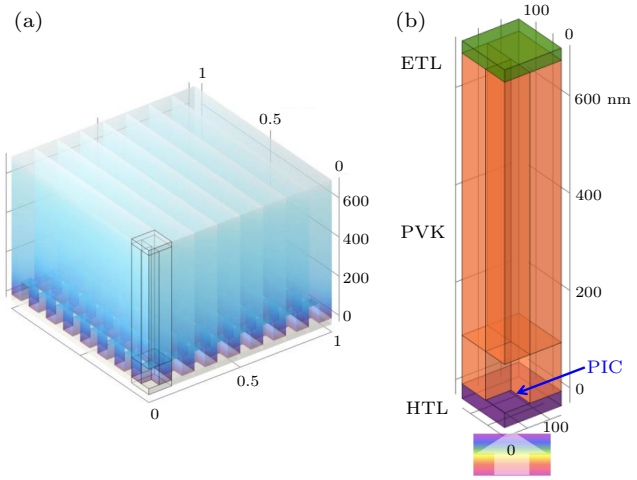



**Fig. 1.** Schematic diagram on perovskite solar cells with PIC structures: (a) 3D model, and (b) unit cell of the 3D model and used into our calculations. The PIC coverage fraction changes with respect to total cross section area.

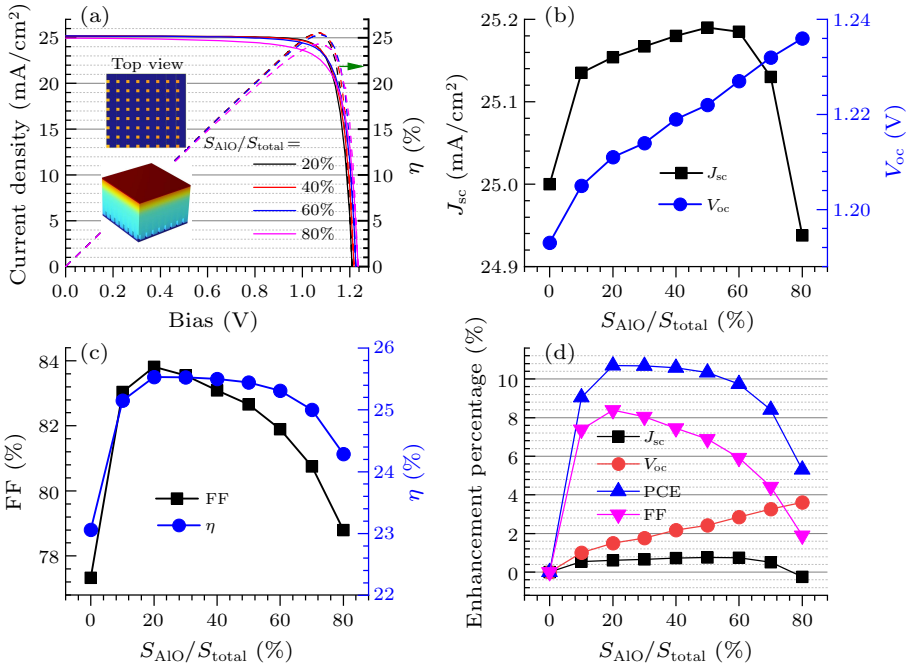



**Fig. 2.** Calculated results using three-dimensional drift-diffusion simulation on perovskite solar cells (p–n–n structure) incorporating porous insulator contact (3D-PIC with $d = 100$ nm and $h = 100$ nm) structures. (a) Curves of current density versus voltage ($J$–$V$) by varying the coverage fraction ($S_{AlO}/S_{total}$) from 10% to 80%. The inset showcases a typical solar cell structure with PICs embedded within it. (b)–(d) $J_{sc}$, $V_{oc}$, FF, PCE and enhancement percentage change versusu PIC's coverage fraction, where difference behaviors could be clearly found and the maximal PCE appears at PIC's coverage fraction of 20%–40%.

## 3. Results

The results of device performance with increasing coverage fraction in three-dimensional PIC nano-structured perovskite solar cells are depicted in Fig. 2. The parameters used the simulation are listed in Table S3 and a few other parameters are mentioned above. The maximum PCE appears at around 20% to 40% PIC coverage, consistent with the experimental observations shown in Fig. 2 of Ref. [1]. Specifically, it was observed that $J_{sc}$, FF, and PCE initially increase with the PIC coverage but then decrease. In contrast, $V_{oc}$ increases during high coverage of PIC due to decreased contact area

and related interface along with fewer total defects. The enhanced percentages of $J_{sc}$, $V_{oc}$, FF, and PCE are summarized in Fig. 2(d), where a $\sim$ 11% PCE improvement was found, which is also consistent with the experimental results by Peng *et al.* Moreover, our calculations emphasize the importance of meticulously preparing high-quality perovskite films with appropriate coverage fractions of $Al_2O_3$. Here, we have carefully examined the effects on energy band diagrams before and after inserting PICs, revealing minimal differences between PVK without PICs and with PICs, as illustrated in Fig. S3 in the supplementary materials . The additional impact of different types of perovskite films (intrinsic and p-type) and the calculations with different dimensions on the final enhancement has also been provided in Figs. S4–S6. It is noteworthy that both intrinsic and p-type perovskites exhibit similar behavior to that observed in n-type perovskite results. Moreover, our calculations suggest that the maximum PCE could reach up to 27.4% when not accounting for any defects either in the bulk material or at the interfaces.

A natural follow-up question is which parameter dominates device performance improvement, since Peng *et al.* pointed out that perovskite solar cells with PICs exhibit the highest $V_{oc} \times$ FF relative to the Shockley–Queisser limit for a p–i–n device. To investigate the key factors contributing to the enhancement of FF and $V_{oc}$, separate studies were conducted on the impact of carriers' mobility and surface defects on $J$–$V$ curves, where the Shockley–Read–Hall (SRH) model has been applied. It is important to notice that the bulk trap densities have already been incorporated in the SRH model.[11] As shown in Fig. 3, the dependence of mobility, carrier recombination lifetime, and defect densities at perovskite/hole transporting layer interfaces was analyzed, revealing clear indications: (i) Increased FF could be mainly affected by perovskite crystallinity-induced carriers' mobility and longer carrier recombination lifetime change (also see Fig. S7); an increase in mobility and carrier recombination lifetime led to an improvement in FF from 75.6% to 84.7%. (ii) Defect densities mainly change the $V_{oc}$ as they strongly affect the splitting of quasi-Fermi levels of electrons and holes ($E_{Fn}$ and $E_{Fp}$),[12,13] while only having a minor influence on FF (which increases only from 84.0% to 86.4%). Peng *et al.* also noted that the inappropriate size of $Al_2O_3$ nanoparticles and non-uniform dispersion concentration could impede performance improvements due to the insulating properties of $Al_2O_3$.[1]

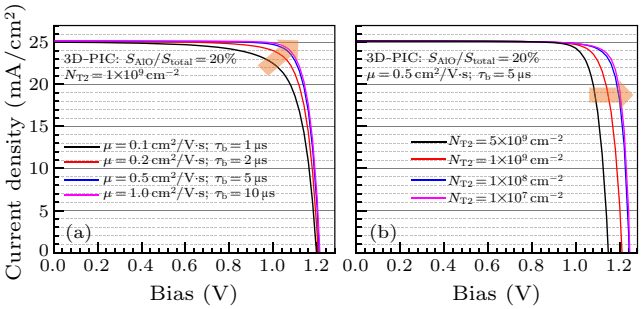



**Fig. 3.** (a) Dependence of mobility and carrier recombination lifetime on device performance, where the fixed surface defects at perovskite/hole transporting layer was given with $N_{T2} = 1 \times 10^9$ cm$^{-2}$, and the coverage fraction ($S_{AlO}/S_{total}$) was exemplarily chosen at 20%. (b) The corresponding $J$–$V$ curves in dependence on surface defects at perovskite/hole transporting layer.

Finally, light trapping, caused by the different refractive indexes between $Al_2O_3$ and perovskite films, leads to a slight increase in $J_{sc}$ (as seen in Fig. 3(b) of Peng *et al.*) and promotes the PCE of PIC-nanostructured perovskite solar cells. An example of the 3D-simulated electromagnetic field distribution ($E_y$) in perovskite solar cells under $\lambda = 624$ nm incident light can be observed in Fig. 4. It shows higher intensity of $E_y$ with the presence of $Al_2O_3$ nanostructures under a coverage fraction ($S_{AlO}/S_{total} = 20\%$). This indicates an increased absorption and thus higher contribution to $J_{sc}$. Figure 4(c) provides a direct comparison of simulated $J$–$V$ curves, which clearly indicate that the presence of $Al_2O_3$ nanostructured PICs slightly promotes the device $J_{sc}$, consistent with the experimental results seen in Fig. 4(b) of Ref. [1]. Table 1 summarizes the detailed results for comparisons.

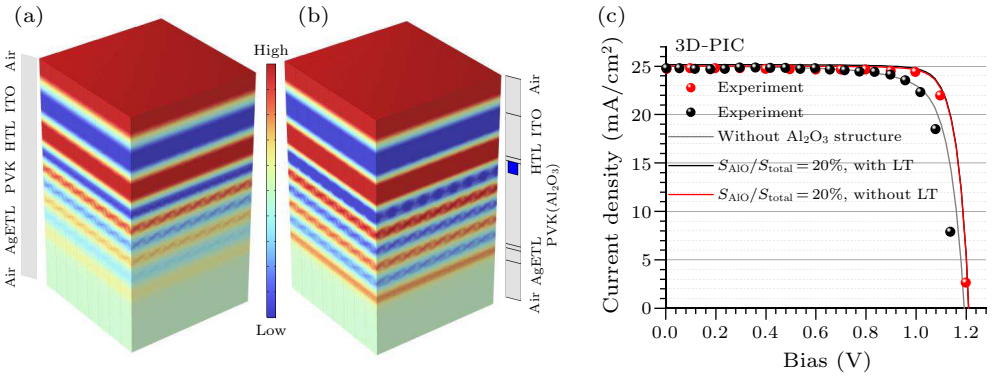



**Fig. 4.** Three-dimensional simulated electromagnetic field distribution ($E_y$) in perovskite solar cells under $\lambda = 624$ nm incident light without (a) and with (b) the $Al_2O_3$ nanostructures under a coverage fraction ($S_{AlO}/S_{total} = 20\%$, 3D-PIC with $d = 100$ nm and $h = 100$ nm). (c) $J$–$V$ curves under three different corresponding conditions (without $Al_2O_3$ nanostructures, with $Al_2O_3$ nanostructures but excluding light trapping (LT), and with $Al_2O_3$ nanostructures including light trapping). The experimental results from Ref. [1] are also incorporated for direct comparisons.

**Table 1.** Calculated results for perovskite solar cells by considering the impact of inserting PIC and related photon recycling (PR).

| 3D | $V_{oc}$(V) | $J_{sc}$ (mA/cm$^2$) | FF (%) | PCE (%) |
|---|---|---|---|---|
| Control | 1.19 | 25.00 | 77.31 | 23.06 |
| PIC without PR | 1.21 | 25.02 | 83.87 | 25.39 |
| PIC with PR | 1.21 | 25.15 | 83.89 | 25.53 |

## 4. Conclusion and perspectives

In light of these considerations, Ref. [1] highlighted that using thick nano-structured PICs in perovskite solar cells can significantly enhance device performance by improving the crystallinity of the perovskite and reducing nonradioactive recombination, the PCE increased from 23% to 25.5% with enhanced bulk recombination lifetime. We have demonstrated that increased mobility, longer carrier recombination lifetime, and effective light-trapping structures are essential in improving device performance, which result in PICs with an area coverage of approximately 25% being able to achieve maximum device performance. Furthermore, the selection of appropriate porous insulator contacts for insertion at the perovskite interfaces not only facilitates surface defect passivation and enhances the quality of the bulk polycrystalline material but may also promote light trapping and absorption within the perovskite films. This approach holds great potential as an effective method for fabricating high PCE perovskite solar cells.

## Acknowledgment

Project supported by the Qing-Lan Project from Yangzhou University and the National Natural Science Foundation of China (Grant No. 62375234). We would like to acknowledge Professor Yadong Xu at Soochow University for the support of electromagnetic simulations. All data is available in the main text or the supplementary materials.

## References

[1] Peng W, Mao K, Cai F, Meng H, Zhu Z, Li T, Yuan S, Xu Z, Feng X, Xu J, McGehee M D and Xu J 2023 *Science* **379** 683

[2] Walter D, Fell A, Wu Y, Duong T, Barugkin C, Wu N, White T and Weber K 2018 *J. Phys. Chem. C* **122** 11270

[3] Jacobs D A, Shen H, Pfeffer F, Peng J, White T P, Beck F J and Catchpole K R 2018 *J. Appl. Phys.* **124** 225702

[4] El-naggar A M, Osman M M, Alanazi A Q, Mohamed M B, Ebdah M A, Aldhafiri A M, Heiba Z K and Albrithen H A 2022 *Appl. Phys. A* **128** 378

[5] Tirado J, Vasquez-Montoya M, Roldan-Carmona C, Ralaiarisoa M, Koch N, Nazeeruddin M K and Jaramillo F 2019 *ACS Appl. Energy Mater.* **2** 4890

[6] Prathapani S, Bhargava P and Mallicka S 2018 *Appl. Phys. Lett.* **112** 092104

[7] Zouhair S, Yoo S M, Bogachuk D, Herterich J P, Lim J, Kanda H, Son B, Yun H J, Wurfel U, Chahboun A, Nazeeruddin M K, Hinsch A, Wagner L and Kim H 2022 *Adv. Energy Mater.* **12** 2200837

[8] Khelifi S, Burgelman M, Verschraegen J and Belghachi A 2008 *Sol. Energy Mater. Sol. Cells* **92** 1559

[9] Pierret R F 1996 *Semiconductor Device Fundamentals* (Reading, MA: Addison-Wesley)

[10] Astakhov O, Carius R, Finger F, Petrusenko Y, Borysenko V and Barankov D 2009 *Phys. Rev. B* **79** 104205

[11] Kandada A D, Innocenzo V, Lanzani G and Petrozza A 2016 *Unconventional Thin Film Photovoltaics* (Royal Society of Chemistry) p. 107

[12] Jin H, Farrar M D, Ball J M, Dasgupta A, Caprioglio P, Narayanan S, Oliver R D J, Rombach F M, Putland B W J, Johnston M B and Snaith H J 2023 *Adv. Funct. Mater.* **33** 2303012

[13] Li H, Xie G, Wang X, Li S, Lin D, Fang J, Wang D, Huang W and Qiu L 2023 *Adv. Sci.* **10** 2300586